

Routing and Link Layer Protocol Design for Sensor Networks with Wireless Energy Transfer

Rahman Doost

Dept. of Electrical and Computer Engineering
Northeastern University
Boston, MA 02115, USA
Email: doost@ece.neu.edu

Kaushik R. Chowdhury

Dept. of Electrical and Computer Engineering
Northeastern University
Boston, MA 02115, USA
Email: krc@ece.neu.edu

Marco Di Felice

School of Computer Science
University of Bologna
Bologna, Italy
Email: difelice@cs.unibo.it

Abstract—Wireless sensor networks are equipped with batteries with limited charge, and are often deployed in conditions that make their retrieval and replacement infeasible. Thus, energy conservation has been a primary consideration for protocol design for such networks. Recent advancements in the transfer of energy wirelessly over large distances, such as through radio frequency electromagnetic (EM) waves and magnetic coupling, may give rise to a new class of networks that allow the sensors to be charged on the field, thereby prolonging the network lifetime. Moreover, wireless charging through EM waves may be undertaken in the same unlicensed band as that used for communication, leading to several unique protocol design challenges for such a network. The contribution of this paper is threefold: First, a set of experiments is undertaken to investigate the effect of distance and location on the energy transfer through EM waves. Second, a new routing metric based on the charging ability of the sensor nodes is proposed. Finally, an optimization framework is developed to determine the optimal charging and transmission cycle for the sensor network, resulting in enhanced lifetime of the network under user-specified end-to-end constraints of throughput and latency.

I. INTRODUCTION

Wireless sensor networks have been the focus of the research community over the past several years leading to protocols and applications suited for scientific data gathering, surveillance, industrial and structural monitoring, military sensing, home metering, among others. Though different applications have varying performance constraints, they are limited by the battery resource on the sensor nodes. Once the residual energy level in the battery falls below a threshold, the sensor can no longer participate in either sensing or packet forwarding tasks, leading to possible network disconnection. We consider a novel approach to this problem, where we allow sensors to be re-charged wirelessly by external radio frequency electromagnetic (EM) waves enabled by an energy transmitter (ET). As the ET must not interfere with the operation of licensed users, it must itself use the unlicensed bands for the energy transfer. Thus, the very action of re-charging a sensor also interferes with the on-going data communication in the neighborhood, necessitating that the sensor cease communication during the charging duration. In this paper, we explore the design of the upper layer protocols, such as the link and routing layers, while evaluating the tradeoffs between allowing sensors to charge, and the network goals of higher throughput

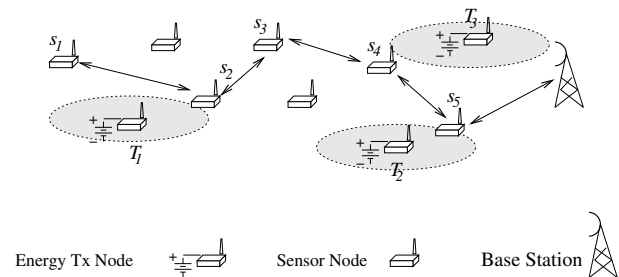


Fig. 1. Network architecture for Energy Harvesting Sensor Networks (EHSNs)

and enhanced lifetime. To the best of our knowledge this is the first work that attempts to experimentally determine the limits of such wireless energy transfer technique with actual off-the-shelf hardware, and use these measurements for end-to-end protocol design.

In our approach, we assume the external device ET serves as a constant power source by either collecting the energy from sources such as solar, vibrational, wind, and biochemical sources [2], or preferably, by direct connection to the AC mains. Sensor nodes are assumed to be equipped with a re-chargable battery, and the ET must supply the energy wirelessly to the receiver unit on the nodes, which in turn feeds the on-board battery. Thus, for every packet transmission or reception, the sensor uses up some of its residual energy, part of which is replenished in the charging durations. In our experiments, we use the Powercaster transmitters to realize the ET and the P2000 series Powerharvester receivers to collect the energy from the EM waves [4].

The network architecture is described in Figure 1, with the sensors deployed randomly in the study area. The ETs are represented by T_1 , T_2 , and T_3 that are connected to a power source. Each of these power transmitters is effective within a coverage region, shown in the figure by shaded circular regions. The placement of these transmitters can be pre-determined, or deployed randomly at the time of placing the sensor nodes. Moreover, as we describe later in Section III, the energy transferring rate is not a monotonically increasing function of distance. Rather, several local wireless channel effects considerably influence which sensor locations are more suited

to this form of EM-based energy transfer. The assumptions of our network architecture closely follow our experimental setup where the charging EM waves are transmitted in the 900 MHz ISM band, which also happens to be the transmission band for the mica2 sensors. In the figure, packets are generated by the source, here s_1 , and are forwarded in a multihop manner to the base station (BS) over the intermediate nodes s_2, \dots, s_5 .

The main contributions of our work are as follows:

- Using off-the-shelf equipment, we measure the performance of EM-based energy transmitters, and the variation in the charging time at the receivers as a function of distance.
- We propose a new routing metric that allows routes to be formed with nodes that have the best energy charging characteristics, and thereby prolong network lifetime.
- For the chosen route, we formulate an optimization function to derive, under network specified bounds of latency and throughput, (i) the charging time (T_{ch}), wherein the sensors do not transmit data but only charge their capacitors from the received EM wave energy, and (ii) transmission time (T_{tx}) in which they are allowed to send and receive data.

The rest of this paper is organized as follows. In Section II we describe the related work, followed by our experimental results in Section III. The routing protocol that leverages the charging ability of the nodes is given in Section IV. In Section V, we describe our charging-transmission optimization framework in detail. We undertake a thorough performance evaluation in Section VI, and finally, Section VII concludes our work.

II. RELATED WORK

Maximizing the steady state data flow from the source node to the destination, under constraints of power, bandwidth, and the rate of harvesting is explored in [8]. The proposed self-adapting maximum flow (SAMF) routing strategy finds feasible paths while automatically adapting to time-varying operating conditions. A geographic routing protocol D-APPOLO for asynchronous energy-harvesting WSNs is proposed in [7]. It periodically and locally calculates the duty-cycle of each node, based on an estimated energy budget for each period which includes the currently available energy, the predicted energy consumption, and the energy expected from the harvesting device assuming solar cells rated at 200 – 300 mWh. The energy aware distance vector routing (EADV) protocol is devised for sensor nodes that are powered by small solar cells and use capacitors for storage [9]. One of the factors influencing the route decision is a cost metric, that is determined by the overhead of gathering the energy. For the capacitor, the quality factor (Q-value) determines the energy loss rate within the device, and therefore routes must be chosen that minimize Q to prevent waste of energy.

At the link layer, there have been several efforts towards identifying optimal charging-transmission cycles. [6] analyzed the requirements for “energy neutral,” i.e., matching energy consumption to production. In this work, the consumption rate

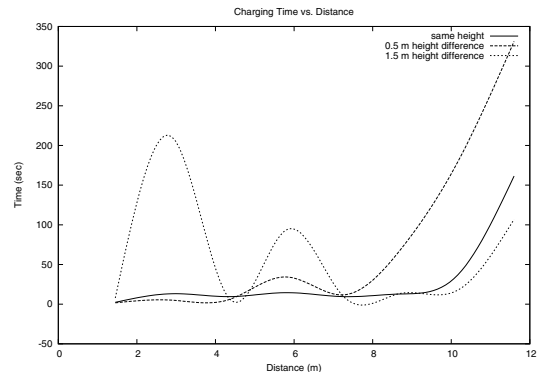


Fig. 2. Variation of the charging time of a capacitor on the receiver as function of increasing distance for different transmitter-receiver heights.

is adapted by changing the duty cycle or the transmit power of the nodes. In addition to dynamic duty cycling algorithms, [5], analyzed the performance of the conventional MAC schemes like CSMA and ID Polling on WSNs with ambient energy harvesting capabilities.

III. EXPERIMENTS WITH EM ENERGY TRANSFER

In this section, we determine experimentally the charging times for a given commercially available wireless energy transfer device, by the following steps:

A. Setup

Our experimental apparatus consists of a P2100 energy harvesting module from Powercast Co. [4], which operates in the 900 MHz ISM band, and is composed of an energy transmitter (ET) and receiver boards. The receiver converts the energy of the transmitted continuous wave 3 W signal sent by the ET to DC voltage with the help of a 1mF capacitor. This stored energy in the capacitor can then be used to re-charge standard batteries as the load, or directly for sensor operation. We compared the charging rates of the capacitor from 0 – 1.16 V, with the latter being a hardware enforced upper limit, for different transmitter-receiver separation distances in the range [1.5, 12] meters. The experiments were conducted in a long corridor of our research building that simulated a tunnel-like behavior. Moreover, at each chosen distance, three different relative heights between the ET and the receiver we chosen as follows: (i) same height, (ii) receiver 0.5 m higher than ET, and (iii) receiver 1.5 m higher than ET, respectively.

B. Observations

The results of our experiments are shown in Figure 2 with the time for charging on the Y-axis, and the separation distance on the X-axis. Firstly, as a limiting condition, we observed that at distances greater than 12 m, the charging takes an infinite length of time, since the capacitor does not get to the maximum charge voltage at all. Thus, we assume this distance as the upper limit for the current type of energy transferring devices. Irrespective of the relative heights between the ET and the receiver, the general trend is towards an increasing charging time with distance. Interestingly, for

1.5 m height difference, there is considerable fluctuation at closer distances. The reason for this is the reflection of the EM waves from the ceiling (as the receiver is placed closer to the ceiling), and peculiar behavior of propagation loss inside a tunnel [1]. This result gives the non-intuitive message that even if a sensor is situated at a greater distance than others, depending upon the location-specific channel behavior, it may still exhibit a better charging rate (e.g. at the distances of 4.5 and 7 m for all the three heights). Note that for different hardware, these times will differ, and with improvements in RF transfer efficiency, the charging times can be significantly improved that can positively affect the network design. We use our experimental findings as a guideline to develop routing and link layer adaptation at the sensor networks using a similar RF transfer apparatus, as described in the next sections.

IV. CHARGING-AWARE ROUTE FORMATION

From our experiments, we observed that the charging rate for a given receiver (which we assume to be placed on a sensor mote, as indicated in Section I) is highly dependent on its specific location and relative height difference with respect to the energy transmitter ET. Thus, classical metrics such as shortest path, in which all nodes are considered to exhibit a homogenous charging characteristic, do not work well in a realistic setting. Moreover, the residual energy at a sensor may vary during the transmission and re-charging process, and hence this too cannot be static metric during route formation. The steps of our routing protocol are given as follows:

A. Route Establishment Metric

We propose using the charging time (2), measured as the time taken to reach the hardware limited voltage of 1.16 V as the decision metric. First, there is an initialization phase, before the start of the network operation. The ETs transmit continuously for a pre-determined duration, allowing each sensor i to measure its own charging time, t_{ch}^i , and the standard deviation η_{ch}^i over multiple trials.

B. Route Formation

The route formation is initiated by the source node, and our proposed metric can be combined with most existing routing protocols for WSNs. In the current implementation, we modify AODV by including the tuple $\langle T_{ch}^{max}(k), \eta_c^{max}h(k) \rangle$ in the route request (RREQ) packet that travels over path k . Here, $T_{ch}^{max}(k)$ represents the maximum charging time considering all the nodes currently traversed in the path k , and $\eta_c^{max}h(k)$ is the observed standard deviation for this maximum value. As the RREQ is forwarded by the sensors, they may update the field $T_{ch}^{max}(k)$ if their own charging time is greater than the value contained in this field. Thus, for a sensor i , the change $T_{ch}^{max}(k) = t_{ch}^i$ if $t_{ch}^i > T_{ch}^{max}(k)$, is undertaken before broadcasting the RREQ to its neighbors. In addition, the deviation $\eta_c^{max}h(k)$ is also included in the packet, whenever the $T_{ch}^{max}(k)$ changes, to resolve the ties at the destination.

To ensure that the best routes deliver the RREQs first, each node introduces a forwarding delay as a function of its own

charging rate. This delay is computed as $t_{ch}^i + \eta_{ch}^i$, i.e. the sum of the mean charging time and its deviation of the node divided by a constant factor (e.g. 1000 for delay in the order of ms).

The destination receives multiples RREQs representing the different paths traversed from the source. It now chooses the path, say ψ , with the lowest value of the maximum charging times of the various paths. Thus,

$$\begin{aligned} \psi &= \min\{T_{ch}^{max}(k)\} \forall k \\ &= \min\{\max[t_{ch}^i]\} \forall i \in \text{path } k, \forall k, \end{aligned} \quad (1)$$

The destination waits for a time T_{setup} during the route formation and collects multiple RREQs. Shorter charging times also imply more opportunity for packet transmission, and results in greater throughput. The per-hop delay incurred in the few additional hops in the chosen path is easily offset by the gains in increased network lifetime, as we show in Section VI. In the next section, we demonstrate how the charging and transmission durations are optimally decided for the selected path while considering several end-to-end performance metrics.

V. CHARGING AND TRANSMISSION TIME OPTIMIZATION

After the base station chooses the optimal path, it sends back the route reply (RREP) to the nodes of this path, defining the charging (T_{ch}) and transmission times (T_x) that is common to all of them. Thus, even if a node i advertised a different value for t_{ch}^i to charge fully, it must now cease transmission and stay in the charging phase for the entire length specified by T_{ch} . Our optimization framework given below returns the duration for charging T_{ch} and the frame length T_{frame} , where $T_{frame} = T_{ch} + T_x$. Once the RREP reaches the source in the return path, all the nodes are initialized and the network can now begin forwarding the data packets.

$$\begin{aligned} \text{Given : } & L_{lim}, ESR_{lim}, N \\ \text{To find : } & T_{ch}, T_{frame} \end{aligned} \quad (2)$$

$$\text{To Maximize : } Throughput = \frac{T_x \cdot R}{T_{frame}}$$

Subject to :

$$(E_{rec} - E_{idle}) \cdot T_{ch} - E_{tx} \cdot T_x \geq 0 \quad (3)$$

$$N \left(T_{ch} + \frac{P + H}{R} \right) \leq L_{lim} \quad (4)$$

$$\frac{1}{ESR_0} \left[1 - k \cdot t \cdot \exp^{-\frac{4700}{T+273}} \right] > \frac{1}{ESR_{lim}} \quad (5)$$

$$T_{frame} = T_x + T_{ch} \quad (6)$$

The aim of this optimization framework is to maximize the throughput subject to several constraints. As the node can only transmit during the transmission times, and must remain silent during the charging times, the throughput is expressed as the ratio of total number of bits sent during T_x to the frame time T_{frame} . The end-to-end latency limit L_{lim} and the capacitor quality metric ESR_{lim} are specified based on application and

device lifetime requirements. Finally, N is the total number of nodes in the path. In order to find the charging time T_{ch} and the frame time T_{frame} that maximizes the throughput, we define the constraints as follows:

- The constraint of keeping the sensor alive after each frame duration is reflected in (3). Here, the sensor expends idle energy E_{idle} during its charging time. This is a function of the internal circuit operation of the sensor. However, it gains energy at the rate E_{rec} from the wireless transmitter in this duration T_{ch} . In addition, during the transmission duration the sensor loses energy at the rate E_{tx} due to sending and receiving packets. Thus, after the frame duration, the residual energy must at least be greater than 0.
- The end-to-end latency of a packet for the N hop route must be below a pre-decided limit L_{lim} as given in (4). This can be function of the type of application and the nature of the data expected from the network. At each hop, in the worst case, a sensor may experience a delay equal to the charging time T_{ch} in which no data can be sent and the transmission delay which is given by the ratio of the packet size P combined with the header size H and the sending rate R .
- Equivalent series resistance (ESR) is a metric that is used to determine the operational quality of the capacitor. Over time, the ESR increases, and once it is beyond the limit ESR_{lim} , the capacitor is considered dysfunctional. The capacitor lifetime constraint is captured in (5), where T is the absolute temperature in Kelvin at which the capacitor operates, t is the operational time, and k is a design constant. The capacitor is subjected to a charging voltage only during the interval T_{ch} in each frame. Thus, if μ is the target network lifetime in terms of number of completed frames, then the effective operational time of the capacitor is $t = \mu \cdot T_{ch}$.
- Finally, the constraint (6) gives the relationship between the charging and transmission times and the frame time.

VI. PERFORMANCE EVALUATION

In this section, we undertake a simulation study of our proposed approach using the ns-2 simulator. We assume that mica2 sensor nodes are deployed with the device parameters for simulation chosen from [10]. These parameters are also listed in Table I. The main reason for this choice is that our experimental readings are for the 900 MHz ISM band, which is also the operational band for the mica2 motes.

Tx Power (mW)	82.23
Rx Power (mW)	45.35
Idle Power (mW)	17.23
Tx Rate (Kbps)	38.4

TABLE I
OPERATIONAL PARAMETERS OF MICA2 MOTES

A total of 500 sensor nodes were randomly deployed in a 300×300 m area. Also, 256 energy transmitters, or ETs,

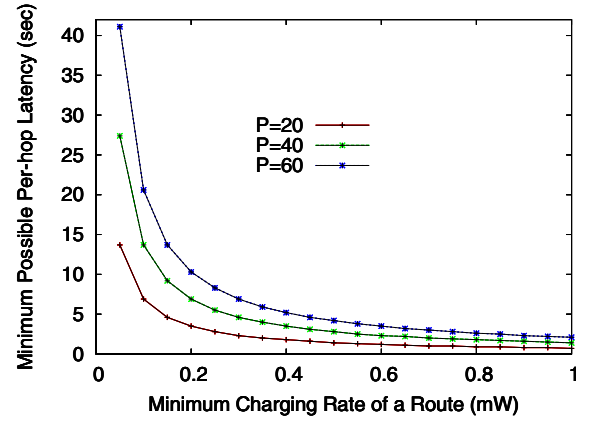


Fig. 3. Results of the optimization equation

are placed in the form of a regular grid, 16 on each row, and separated by 20 m each. This density allows each node to fall within the coverage range of exactly one ET. In this study, we vary the sensor packet sizes, from 20 to 80 bytes, in increments of 20 bytes. The value of T_{ch} , the optimal charging time obtained from the optimization is used to demonstrate the benefits of our approach. In addition, we introduce a factor $0 < k \leq 1$, which will be used to scale down the optimal charging time T_{ch} for different set of trials. Thus, the simulation considers 4 different values of k , i.e., 0.25, 0.5, 0.75 and 1.0, with the intention of studying how the choice of a small charging time affects the performance. The values of ESR_{lim} and ESR_0 are set at 300 and 0.3, respectively as per industry specifications.

The nodes have a charging behavior similar to the actual experiments, as shown in Figure 2. Since the time to fully charge exhibited some temporal variations in our experiments, each node, say i , chooses a value with a uniform distribution within the interval $[t_{ch}^i - \eta_{ch}^i, t_{ch}^i + \eta_{ch}^i]$, where t_{ch}^i and η_{ch}^i are the average and deviation of the node's capacitor's charging time. The initial energy of the system is set to 100 mJ which gets decremented after transmission or reception, and incremented by the charging value at the end of each cycle.

Equation (4) sets an upper bound L_{lim} on the end-to-end latency of packets for an N -hops route. By choosing a value of the charging time necessary for the transmission of at least one packet, we derive the relationship between L_{lim} and the rate of charging of the nodes. If L_{lim} is too tight, then either the node will not be able to charge enough or a node may not be alive after each transmission (Equation (4)). In Figure 3, we show the lowest possible values of L_{lim} on the Y-axis that can be set in the optimization problem for different values of the charging rate E_{rec} and packet sizes.

Figures 4(a) and 4(b) show the average end-to-end throughput and network lifetime, respectively, for 50 runs of simulation with different values of k and packet sizes. Figure 4(a) implies that by considering values of the charging time lower than the optimal derived T_{ch} , the throughput of the network increases greatly. However, the penalty occurs in lifetime of

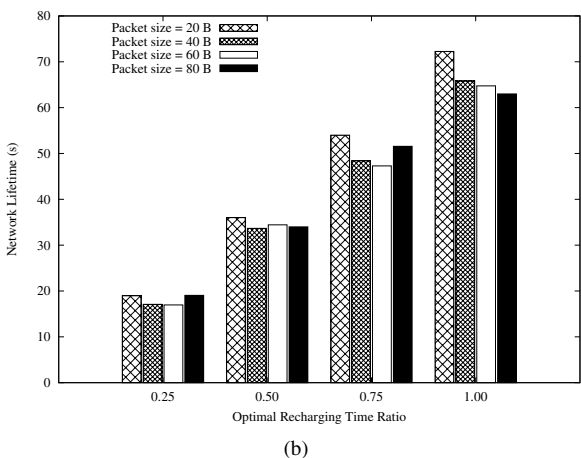
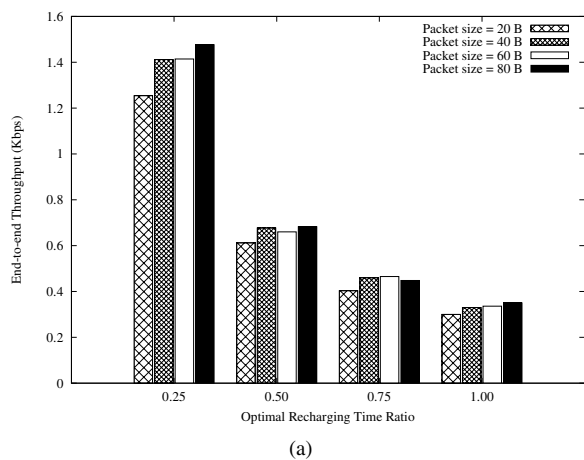


Fig. 4. The end-to-end throughput (a) and the network lifetime (b) for different packet sizes measured against increasing charging time ratio.

the network which shows a near-linear decrease. However, the rate at which the throughput increases exhibits a non-linear curve, thus hinting that for sudden high bandwidth needs, decreasing the recharging time (thereby increasing the transmission time) will not incur a proportionally high degradation of lifetime. Moreover, we observe that different packet sizes do not impact the performance significantly. This occurs because of the design of our optimization problem. Thus, each node has sufficient charging duration to collect energy for transmission of at least one packet during its transmission time, which in turn is proportional to the packet size.

Figure 5 shows the residual energy of the source node in the path. The effect of design factor k (i.e. fractional reduction of optimal T_{ch}) is reflected in this plot to show how fast this node dies with different k 's. With longer recharging cycles the amount of added energy to the system increases, and reaches closer to the energy which is about to be consumed in the next transmission cycle. Since the recharging value at each cycle is random, so is the difference between consecutive energy addition and consumption in a frame. This gives rise to some minor variation in the energy reduction rate of the system. The slight knees observed in the curves corresponding to $k = 0.75$

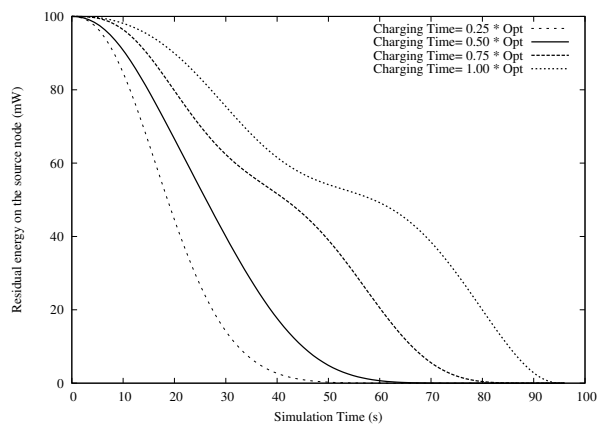


Fig. 5. Residual energy at the source node as function of simulation time.

and $k = 1.0$ are a reflection of this effect.

VII. CONCLUSIONS

In this paper, we have taken the first steps towards identifying the network protocol challenges when the sensors are charged wirelessly in the same frequency band as that used for communication. We have shown that paths based on simple metrics such as hop count may not be suitable for such networks. Through experimental tests, we verified the dependence on location and distance on the charging ability of the nodes, and proposed a link layer optimization framework that best addresses the tradeoff of charging and transmission durations. Further work will be undertaken by a complete network implementation and testing under real-world conditions.

REFERENCES

- [1] I. F. Akyildiz, Z. Sun and M.C. Vuran, Signal Propagation Techniques for Wireless Underground Communication Networks. Physical Communication (Elsevier) Journal, vol. 2, no. 3, 167–183, September 2009.
- [2] J. A. Paradiso and T. Starmer, Energy Scavenging for Mobile and Wireless Electronics. *IEEE Pervasive Computing*, vol. 4, no. 1, Jan 2005.
- [3] C. R. Murthy, Power Management and Data Rate Maximization in Wireless Energy Harvesting Sensors. *Int J Wireless Inf Networks*, vol. 16, pp. 102117, September 2009.
- [4] Powercast Corporation, P2000 Series 902 – 928 MHz Powerharvester Development Kit. [Online] <http://www.powercastco.com/products/development-kits/>
- [5] Z. A. Eu, W. K. Seah, and H. Tan, A Study of MAC Schemes for Wireless Sensor Networks powered by Ambient Energy Harvesting. *ACM Intl. Conf. on Wireless Internet*, pp. 1–9, Maui, Hawaii, November 2008.
- [6] A. Kansal, J. Hsu, S. Zahedi, and M. B. Srivastava, “Power Management in Energy Harvesting Sensor Networks,” *ACM Trans. on Embedded Computing Systems*, vol. 6, no. 4, September 2007.
- [7] D. Noh, I. Yoon, and H. Shin, “Low-Latency Geographic Routing for Asynchronous Energy-Harvesting WSNs,” *Journal of Networks*, pp. 78–85, vol. 3, no. 1, January 2008.
- [8] A. Bogliolo, S. Delpriori, E. Lattanzi, A. Seraghiiti, “Self-adapting Maximum Flow Routing for Autonomous Wireless Sensor Networks,” *Springer Cluster Computing Journal*, to appear, 2010.
- [9] S. Mahlkecht, S. A. Madani, and M. Roetzer, “Energy Aware Distance Vector Routing Scheme for Data Centric Low Power Wireless Sensor Networks,” *IEEE Intl. Conf. on Industrial Informatics*, pp. 1030 - 1035, August 2006.
- [10] M. Calle and J. Kabara, Measuring Energy Consumption in Wireless Sensor Networks Using GSP. in *Proc. of IEEE PIMRC*, Helsinki, Finland, 2006.